

RESEARCH

Open Access



Chemogenetic activation of locus coeruleus neurons ameliorates the severity of multiple sclerosis

Alejandro Torrillas-de la Cal^{1,2,3†}, Sonia Torres-Sanchez^{1,2,3†}, Lidia Bravo^{1,2,3}, Meritxell Llorca-Torralba^{2,3,4}, Jose Antonio Garcia-Partida^{1,2,3}, Ana I. Arroba^{3,5} and Esther Berrocoso^{1,2,3*}

Abstract

Background Most current disease-modifying therapies approved for multiple sclerosis (MS) are immunomodulatory drugs that counteract the aberrant activity of the immune system. Hence, new pharmacological interventions that drive anti-inflammatory activity and neuroprotection would represent interesting alternative therapeutic approaches or complementary strategies to treat progressive forms of MS. There is evidence of reduced noradrenaline levels and alterations to locus coeruleus (LC) noradrenergic neurons in MS patients, as well as in animal models of this disease, potentially factors contributing to the pathophysiology. Drugs that enhance noradrenaline appear to have some beneficial effects in MS, suggesting their potential to dampen the underlying pathology and disease progression.

Methods Therefore, we explored the consequences of chronic LC noradrenergic neurons activation by chemogenetics in experimental autoimmune encephalomyelitis (EAE) mice, the most widely used experimental model of MS. LC activation from the onset or the peak of motor symptoms was explored as two different therapeutic approaches, assessing the motor and non-motor behavioral changes as EAE progresses, and studying demyelination, inflammation and glial activation in the spinal cord and cerebral cortex during the chronic phase of EAE.

Results LC activation from the onset of motor symptoms markedly alleviated the motor deficits in EAE mice, as well as their anxiety-like behavior and sickness, in conjunction with reduced demyelination and perivascular infiltration in the spinal cord and glial activation in the spinal cord and prefrontal cortex (PFC). When animals exhibited severe paralysis, LC activation produced a modest alleviation of EAE motor symptoms and it enhanced animal well-being, in association with an improvement of the EAE pathology at the spinal cord and PFC level. Interestingly, the reduced dopamine beta-hydroxylase expression associated with EAE in the spinal cord and PFC was reversed through chemogenetic LC activation.

Conclusion Therefore, clear anti-inflammatory and neuroprotective effects were produced by the selective activation of LC noradrenergic neurons in EAE mice, having greater benefits when LC activation commenced earlier. Overall, these data suggest noradrenergic LC neurons may be targets to potentially alleviate some of the motor and non-motor symptoms in MS.

[†]Alejandro Torrillas-de la Cal and Sonia Torres-Sanchez contributed equally to this work and share first authorship.

*Correspondence:

Esther Berrocoso
esther.berrocoso@uca.es

Full list of author information is available at the end of the article



© The Author(s) 2023. **Open Access** This article is licensed under a Creative Commons Attribution 4.0 International License, which permits use, sharing, adaptation, distribution and reproduction in any medium or format, as long as you give appropriate credit to the original author(s) and the source, provide a link to the Creative Commons licence, and indicate if changes were made. The images or other third party material in this article are included in the article's Creative Commons licence, unless indicated otherwise in a credit line to the material. If material is not included in the article's Creative Commons licence and your intended use is not permitted by statutory regulation or exceeds the permitted use, you will need to obtain permission directly from the copyright holder. To view a copy of this licence, visit <http://creativecommons.org/licenses/by/4.0/>. The Creative Commons Public Domain Dedication waiver (<http://creativecommons.org/publicdomain/zero/1.0/>) applies to the data made available in this article, unless otherwise stated in a credit line to the data.

Keywords Multiple sclerosis, Experimental autoimmune encephalomyelitis, Locus coeruleus, Noradrenaline, Spinal cord

Introduction

Multiple sclerosis (MS) is a chronic neurological autoimmune disease that is estimated to affect 2.8 million people worldwide and it represents the leading cause of non-traumatic disability in young adults [1–3]. This pathology affects the central nervous system (CNS) and it produces progressive irreversible demyelination, with severe motor and non-motor consequences [4]. While most current disease-modifying therapies approved for MS are immunomodulatory drugs, mainly aimed at decreasing the frequency of relapses, they have a limited efficacy in halting disease progression [5]. Hence, other pharmacological interventions that effectively drive anti-inflammatory and neuroprotective effects would represent an alternative or additional therapeutic approach to treat MS.

There is evidence that disruptions to physiological noradrenaline homeostasis or signaling might contribute to MS. Indeed, impaired noradrenergic functional connectivity and axonal damage in the locus coeruleus (LC), the main source of noradrenaline in the CNS, has been reported in MS patients [6–8]. Significant astroglial activation in and around the LC, as well as a reduction in LC noradrenaline levels, have also been reported in human post-mortem brains [9]. In the experimental autoimmune encephalomyelitis (EAE) mice model of MS, neuronal damage in the LC and an associated reduction in cortical and spinal cord noradrenaline levels have also been observed [9], reflecting the disease-induced neuronal harm in the LC. Moreover, damage to noradrenergic LC neurons appears to exacerbate the symptomatology in this animal model [10] although not in others [11–13]. These findings clearly point to altered LC physiology in MS that specifically affects noradrenergic neurotransmission. Interestingly, studies *in vitro* and *in vivo* have demonstrated that noradrenaline restricts the development of neuroinflammatory activation in the CNS, providing neurotrophic support to neurons and protecting astrocytes, microglia and neurons against oxidative stress [14–17]. Furthermore, central noradrenaline acts as a classic neurotransmitter, critically regulating arousal, attention, anxiety and pain [18–21], relevant non-motor behaviors affected in MS.

Interestingly, as there is no clear loss of LC neurons in MS, as in other neurodegenerative diseases like Alzheimer's or Parkinson's disease [22–25], promoting the activity of the LC noradrenergic system might be a therapeutic option in MS. However, the consequences of enhancing the availability of endogenous noradrenaline

remain unclear. For example, administering atomoxetine (a noradrenaline reuptake inhibitor) to EAE mice that are already ill does not promote recovery [10], although when administered along with the synthetic noradrenergic precursor L-threo-3,4-dihydroxyphenylserine (L-DOPS), clinical improvements in EAE mice were evident [10]. In MS patients, treatment with noradrenaline reuptake inhibitors (lofepramine or maprotiline) combined with levodopa (which after conversion to dopamine metabolizes to noradrenaline) have been reported to have beneficial effects. However, as dopamine itself exerts beneficial effects on the disease [26], the rise in central noradrenaline levels may not drive these effects. Furthermore, the combination of lofepramine and L-phenylalanine (a precursor of noradrenaline) was initially shown to dampen the clinical symptoms of MS [27], although subsequent studies raised doubts about this therapeutic effect [28]. Therefore, it remains unclear whether limiting neuron damage in the LC or enhancing LC neuronal activity might combat the progression of MS. Indeed, such a therapeutic approach might fail to address the peripheral cardiovascular noradrenergic effects or even peripheral pro-inflammatory actions [29, 30].

Chemogenetic tools, like designer receptors exclusively activated by designer drugs (DREADD), can be used to specifically modulate the activity of LC noradrenergic neurons [31]. Hence, we have explored whether chronic chemogenetic activation of LC noradrenergic neurons has a beneficial effect on the clinical course of EAE, evaluating motor and non-motor behavioral changes as EAE progresses. Furthermore, we studied the effects of this manipulation on demyelination, inflammation and glial activation in the spinal cord and cerebral cortex in the chronic phase of the EAE model. To evaluate the ability of this therapeutic strategy to prevent or restore the alterations induced in the EAE model, chronic chemogenetic activation was first induced from the onset of the disease or at the peak of the motor symptoms, respectively.

Materials and methods

A more detailed description of the experimental procedures is provided in the Additional file 1.

Animals, experimental design and groups

Female C57BL/6 J TH:Cre mice were used in these studies and maintained under standard laboratory conditions at the University of Cadiz. The TH:Cre founders were

provided by INFRAFRONTIER/EMMA (EM:00254) [32]. The Cre-dependent DREADD virus was injected bilaterally into the LC and 10 days later, EAE was induced and the clinical symptoms were monitored from day 7 post-induction (dpi). For chronic chemogenetic LC activation, clozapine-N-oxide (CNO, 3 mg/kg) was administered orally on a daily basis from the onset (~12 dpi) or the peak of motor symptoms (peak phase of EAE: clinical score ≥ 3 , ~17 dpi). The animals were then killed in the chronic phase of EAE (from ~20 dpi), collecting the spinal cord and brain tissues at 27–29 dpi to assess the neurobiological alterations (Figs. 1A, 5A). The experimental groups established in this study were control animals (naïve group), and groups of EAE animals administered a control-DREADD or rM3D(Gs)-DREADD into the LC (EAE and EAE-rM3D groups, respectively) and treated chronically with CNO or the vehicle alone.

DREADD virus injection

Mice were injected with a DREADD virus (rM3D(Gs)-DREADD or control-DREADD) bilaterally into the LC (AP – 5.3 mm, ML \pm 1 mm, – 3.6 mm from the surface of the skull) [33] and DREADD expression in the LC was verified at the end of the experiments (Additional file 1: Fig. S1).

EAE induction and evaluation

Mice were immunized by subcutaneous injection of mouse myelin oligodendrocyte glycoprotein peptide (MOG_{35–55}) in complete Freund's adjuvant (CFA), and pertussis toxin (PTX) was then administered intraperitoneally, 2 and 24 h after immunization (Hooke Laboratories Inc, USA). Clinical signs of EAE were assessed daily obtaining a clinical score of 0–4.5. The area under the curve (AUC) values of this score, the maximum score achieved and the relative change in the clinical score at the peak (17 dpi) and in the chronic (25 dpi) phase of EAE (relativized to EAE group at the peak phase) were also analyzed. Body weight was also monitored every 2 days.

Open field test

Mice were placed individually in a square arena (45 × 45 × 35 cm) for 5 min to allow them to explore the space freely. Spontaneous locomotor activity was measured as the total distance travelled, expressed in arbitrary units (AU), as well as the AUC values of the total distance travelled. The time spent in the central area of the arena was also measured as a readout for anxiety-like behavior. To evaluate “sickness behavior”, the time spent in a specific sedentary posture and the activity/attention score were also assessed [34].

Histological and immunohistochemical assays

Hematoxylin–eosin staining was performed on the spinal cord to evaluate the degree of perivascular infiltration [35, 36]. Immunohistochemistry and immunofluorescence assays were carried out to assess the expression of tyrosine hydroxylase (TH) and glial fibrillary acidic protein (GFAP) in the LC, and the co-expression of mCherry (the DREADD reporter protein) and dopamine beta-hydroxylase (DBH) in the LC, A5 and A7. In addition, the expression of myelin basic protein (MBP), GFAP, ionized calcium-binding adapter molecule 1 (Iba1), arginase-1 (Arg1), inducible nitric oxide synthase (iNOS) and DBH were evaluated in the spinal cord, the prefrontal cortex (PFC): prelimbic (PL) and infralimbic (IL) and motor cortices: secondary (M2) and primary (M1). Detailed information about antibodies used is included in Additional file 1: Table S1. Images were acquired on an Olympus BX60 microscope (Olympus, Spain) or a confocal Zeiss LSM 880 (Carl Zeiss Microscopy GmbH, Germany) and analyzed with Fiji Imaging software (USA).

Statistical analysis

The data are represented as the means + standard error of the mean (SEM) and the results were analyzed with a Student's t-test, one- or two-way, or repeated measures ANOVA, followed by Bonferroni or Dunnett's post hoc tests. For non-parametric data, Mann–Whitney *U* or

(See figure on next page.)

Fig. 1 Chronic LC activation from the onset of motor symptoms affects EAE-induced behavioral changes. **A** Experimental timeline showing the design of the study to assess the effect of chronic LC activation from the onset of motor symptoms in EAE. Representative images showing mCherry (red) expression in DBH (green) in the LC. Scale bars: 100 μ m. **B** Clinical score recorded daily through the course of EAE and their area under the curve (AUC) from the onset of motor deficit and CNO administration (shaded area). **C** The severity of EAE is expressed as the maximum clinical score achieved and **D** the percentage change relative to the 17 dpi EAE group, for both the peak (17 dpi) and the chronic (25 dpi) phases of EAE. **E** Body weight over the course of EAE expressed as the relative change from baseline (at the beginning of experiments) and that at the end of experiments (27 dpi). **F** Representative activity traces (chronic phase) and the spontaneous locomotor activity expressed as the total distance travelled (arbitrary units, AU), and the AUC from the onset of motor deficit and CNO administration (shaded area). **G** Representative heat maps (chronic phase) and the relative time spent in the central area of the arena before the onset of motor deficit and CNO administration (10 dpi), and at the peak (17 dpi) and chronic (25 dpi) phases of EAE. **H–J** Activity/attention score (above) and time spent in the sedentary posture (below) at **H** the onset, **I** and at the peak (17 dpi) and **J** in the chronic (25 dpi) phase of EAE. The data represent the mean + SEM and each point corresponds to an individual mouse ($n = 8–10$ per group). # $p < 0.05$, ## $p < 0.01$, ### $p < 0.001$ EAE versus naïve; * $p < 0.05$, ** $p < 0.01$, *** $p < 0.001$ EAE-rM3D_{onset} versus EAE; § $p < 0.05$ EAE-rM3D_{onset} 25 dpi versus 17 dpi (Additional file 1: Table S2). Some elements of this figure were created with [BioRender.com](https://www.bio-render.com)

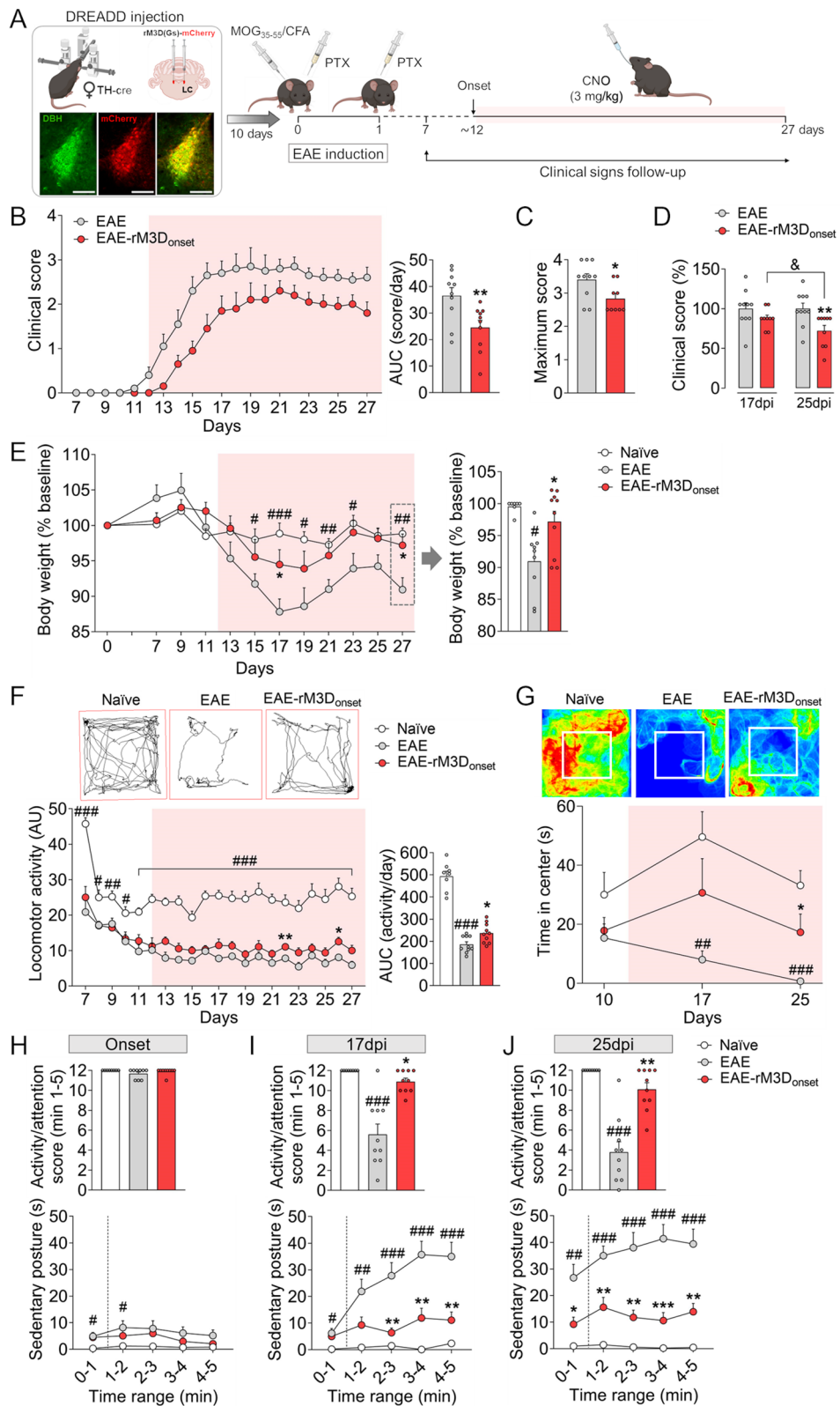


Fig. 1 (See legend on previous page.)

Kruskal–Wallis tests were applied, followed by a Dunn's post hoc test. Correlations were assessed using Pearson or the non-parametric Spearman correlation coefficients. Significance was accepted at $p < 0.05$ (see Additional file 1: Tables S2–S11 for more details on the statistical analysis).

Results

EAE-induced changes in the LC

The possible alterations to the LC induced by EAE were first assessed and a significant increase in the area occupied by GFAP was evident in the EAE mice compared to the naïve animals ($p < 0.05$; Additional file 1: Fig. S2A, B, D). By contrast, no differences were found in the number of cells expressing TH in the LC (Additional file 1: Fig. S2A–C).

The behavioral effects of rM3D(Gs)-DREADD_{onset}-mediated LC activation

In order to assess the effect of chronic LC activation from the onset of the motor symptoms in EAE animals (~12 dpi), we evaluated the animal's motor deficit daily from 7 dpi based on their clinical score. A significant effect on the clinical score was observed through a reduction in the AUC and a lower maximum score in the EAE-rM3D_{onset} animals relative to the EAE mice ($p < 0.01$ and $p < 0.05$, respectively; Fig. 1B, C). Disease severity was expressed as the relative change in the clinical score, which was lower in EAE-rM3D_{onset} compared with control EAE animals in the chronic phase ($p < 0.01$) and with EAE-rM3D_{onset} in the peak phase ($p < 0.05$; Fig. 1D). EAE animals suffered a significant loss in body weight along the disease course, but this was counteracted by LC activation in the EAE-rM3D_{onset} mice ($p < 0.05$; Fig. 1E).

Given that motor dysfunction affects locomotor activity in EAE animals, we tracked their spontaneous locomotor activity daily in an open field from 7 dpi, assessing the total distance travelled. As expected, EAE groups reduced their locomotor activity throughout the follow-up period relative to the naïve animals, with a decrease in the AUC ($p < 0.001$; Fig. 1F). However, chronic LC

activation significantly improved the locomotor activity of EAE mice (AUC, $p < 0.05$; Fig. 1F). A subsequent analysis of the time spent in the center or the periphery of the open field highlighted the significant reduction in the time spent in the former at the peak (17 dpi) and in the chronic (25 dpi) phase of the disease (both $p < 0.01$; Fig. 1G). Interestingly, EAE-rM3D_{onset} mice spent significantly more time in the center of the field in the chronic phase (25 dpi: $p < 0.05$; Fig. 1G). The activity/attention score was also assessed as a parameter reflecting the rodent's sickness. The EAE mice spent more time in a sedentary posture relative to the naïve animals at the onset (min 0–1 and 1–2, $p < 0.05$; score: $p > 0.05$; Fig. 1H) and more robustly at the peak and in the chronic phase of EAE (score: 17 dpi and 25 dpi: $p < 0.001$; Fig. 1I, J). However, EAE-rM3D_{onset} animals spent less time in this sedentary posture relative to the EAE mice, exhibiting a higher score at both the peak and in the chronic phase (score: 17 dpi: $p < 0.05$ and 25 dpi: $p < 0.01$; Fig. 1H–J).

The effects of rM3D(Gs)-DREADD_{onset}-mediated LC activation in the spinal cord

MBP immunoreactivity in the ventral spinal cord white matter was analyzed in the chronic phase of the disease to explore demyelination (Fig. 2A, B). In EAE mice there was a broader area of demyelination than in naïve animals ($p < 0.001$; Fig. 2B), but this was reduced significantly in EAE-rM3D_{onset} animals ($p < 0.001$; Fig. 2B). Peripheral cell infiltration was also explored and as expected, clusters of infiltrates were found in the thoracic spinal cord parenchyma of EAE mice, next to venules ($p < 0.001$; Fig. 2C, D). However, chronic activation of LC noradrenergic neurons in the EAE-rM3D_{onset} mice reduced the penetration of these infiltrates along the parenchyma of the thoracic spinal cord relative to the EAE mice ($p < 0.001$; Fig. 2D). Perivascular cuffs were also studied to determine if the infiltrates penetrate the parenchyma (Fig. 2E) and many perivascular cuffs were evident in EAE animals when compared to the naïve mice ($p < 0.001$; Fig. 2F). Fewer perivascular cuffs were found in EAE-rM3D_{onset} mice ($p < 0.001$; Fig. 2F) and

(See figure on next page.)

Fig. 2 Chronic LC activation from the onset of motor symptoms affects EAE-associated damage in spinal cord. **A** Representative images showing the demyelination in the lumbar spinal cord (cyan, MBP) and **B** its quantification, expressed as the percentage of area free of MBP in the ventral white matter. **C–G** Perivascular infiltration in the thoracic spinal cord analyzed from **C, E** hematoxylin and eosin staining images and reflected as the **D** infiltration score, **F** perivascular cuffs and **G** preclinical cuffs. **H–J** Representative images showing astrocyte activation in the **H** dorsal and **I** ventral horns (DH, VH) of the lumbar spinal cord and a graph of the **J** GFAP immunoreactivity (arbitrary units, AU). **K** Representative immunofluorescence images showing Iba1 (green) expression in the lumbar spinal cord and **L** its quantification, expressed as the relative area of the ventral white matter expressing Iba1. **M–O** Representative immunofluorescence images of Arg1 (red) and Iba1 (green) and corresponding magnifications in the lumbar spinal cord and **P** their quantification, expressed as the percentage of area of the ventral white matter in which Arg1 and Iba1 co-localize relative to the total area occupied by Iba1. The data represent the mean + SEM and each point corresponds to an individual mouse except for **P** that represents a section ($n = 5$ per group except for **P**, 15 sections/animal ($n = 3–4$)). ### $p < 0.001$ EAE versus naïve; * $p < 0.05$, ** $p < 0.01$, *** $p < 0.001$ EAE-rM3D_{onset} versus EAE (Additional file 1: Table S3). Scale bars: **A, K**, 200 μm ; **C, E, H, I**, 100 μm ; (**M, N, O**), 50 μm . 250 μm magnification for the insets in **C**

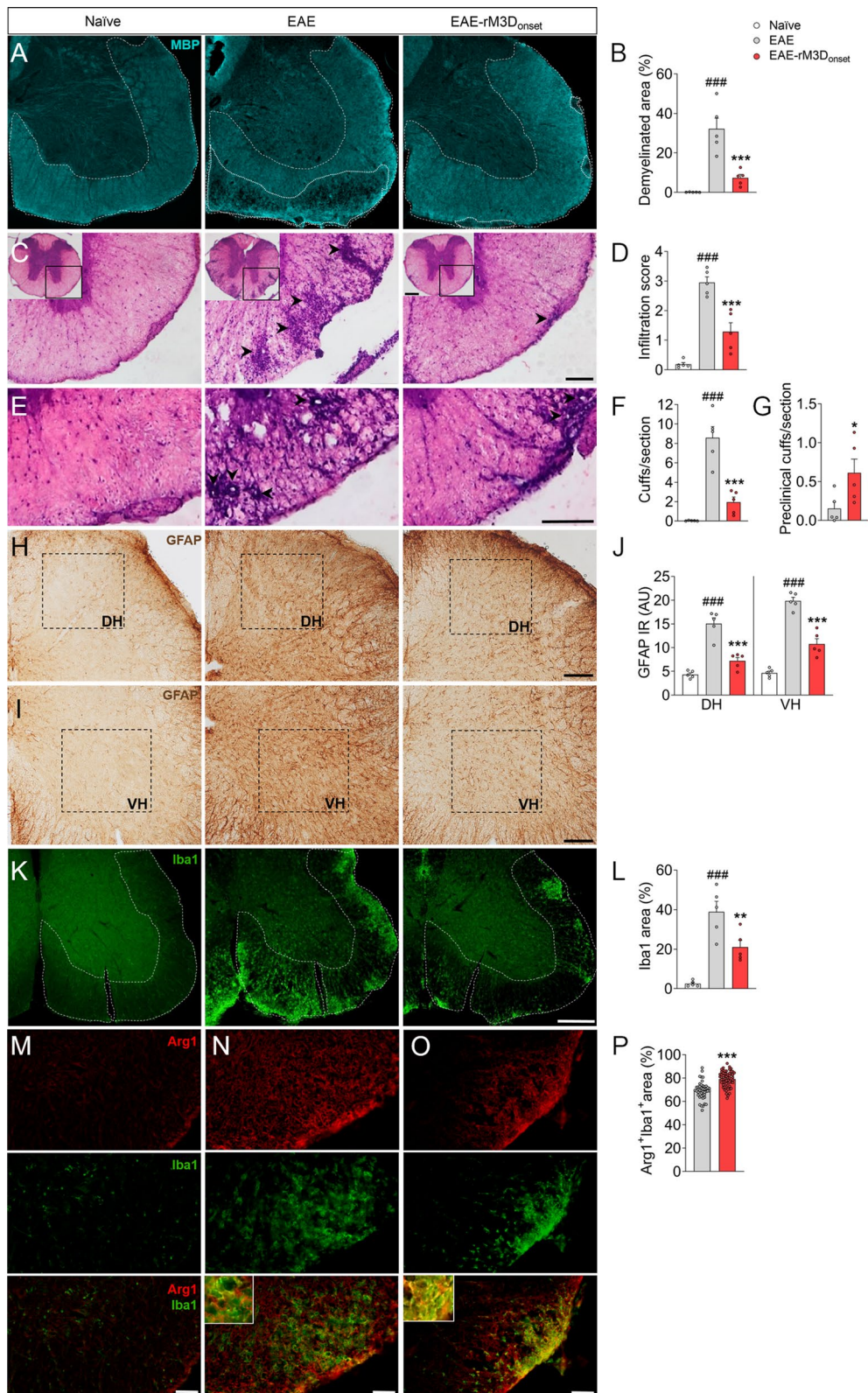


Fig. 2 (See legend on previous page.)

more of them failed to penetrate the parenchyma (preclinical cuffs) than in EAE animals ($p < 0.05$; Fig. 2G).

Glial activation was also explored in the dorsal horn (DH) and ventral horn (VH) of the lumbar spinal cord (Fig. 2H–L), and the stronger GFAP immunoreactivity in the EAE animals' lumbar spinal cord relative to the naïve animals (DH: $p < 0.001$; VH: $p < 0.001$; Fig. 2J) was significantly dampened in the EAE-rM3D_{onset} mice (DH: $p < 0.001$; VH: $p < 0.001$; Fig. 2J). Furthermore, there was an increase in the relative area occupied by Iba1 in EAE mice relative to naïve animals ($p < 0.001$; Fig. 2K, L), which was reduced by LC activation in the EAE-rM3D_{onset} animals ($p < 0.01$; Fig. 2L). The expression of the pro-inflammatory iNOS or the predominantly anti-inflammatory marker Arg1 were evaluated in the regions expressing Iba1. On the one hand, no iNOS immunoreactivity was found in naïve animals, yet residual iNOS expression in perivascular infiltration areas was found in both EAE and EAE-rM3D_{onset} animals but not co-localized with Iba1 (Additional file 1: Fig. S3A–C). Conversely, significant Arg1 expression was evident in the lumbar spinal cord white matter (Fig. 2M–O), which highly co-localized with Iba1 in EAE-rM3D_{onset} mice than in EAE animals ($p < 0.001$; Fig. 2P).

The effects of rM3D(Gs)-DREADD_{onset}-mediated LC activation in the cerebral cortex

Demyelination was also explored in the PFC and motor cortices, yet no differences were found in MBP expression in these areas in the chronic phase of EAE (Additional file 1: Fig. S4A–F). In terms of glial activation (Fig. 3A–D), increased GFAP expression was evident in the IL of EAE animals relative to naïve mice ($p < 0.001$; Fig. 3B) and this was reduced significantly in EAE-rM3D_{onset} mice (IL: $p < 0.05$; Fig. 3B). In the motor cortex, increased GFAP expression was evident in the M2 of EAE mice relative to the naïve animals ($p < 0.01$), but no differences were found when compared to the EAE-rM3D_{onset} mice (Fig. 3D). Regarding Iba1 expression (Fig. 3E–J), no significant differences were observed in the area of the PFC or motor cortices occupied by Iba1 in EAE animals relative to the naïve or EAE-rM3D_{onset} groups (Fig. 3G, J). Although neuroinflammation is not widespread in these cortices, we found basal activation of microglia (Iba1⁺ cells) in these brain areas but no amoeboid or macrophage-like cells were observed.

The effect of rM3D(Gs)-DREADD_{onset}-mediated LC activation on noradrenergic projections

DBH expression in the lumbar spinal cord was reduced all along the spinal cord gray matter in EAE animals (Fig. 4A, B) and in particular, there was a significant reduction in DBH in both the DH and VH of EAE animals relative to the naïve mice (DH: $p < 0.001$; VH: $p < 0.001$; Fig. 4C), which was reversed in the lumbar spinal cord DH by LC activation ($p < 0.01$; Fig. 4C). Like the spinal cord, there was weaker DBH expression in the PL and IL of EAE mice relative to the naïve animals ($p < 0.05$), which was significantly reversed in the IL of EAE-rM3D_{onset} mice ($p < 0.05$; Fig. 4E). Notably, no significant reduction in DBH expression was evident in the motor cortex of the EAE animals (Fig. 4G). The changes in DBH expression correlated well with GFAP immunoreactivity (Additional file 1: Fig. S5A–F) and there appeared to be a significant negative correlation between these markers in the DH and VH of the spinal cord (both $p < 0.01$), and in the IL ($p < 0.05$).

The behavioral effects of rM3D(Gs)-DREADD_{peak}-mediated LC activation

The effect of chemogenetic LC activation was explored from the peak of motor symptoms (~17 dpi), when animals exhibited robust hind limb paralysis (Fig. 5A). In terms of the clinical signs, no significant differences were found in the motor symptomatology of the EAE-rM3D_{peak} mice relative to the EAE animals during the development of the disease, or even in the AUC and the maximum score attributed to these animals (Fig. 5B, C). However, the clinical score of EAE-rM3D_{peak} animals was significantly lower in the chronic phase (25 dpi, $p < 0.001$; Fig. 5D), indicating an improvement to the motor deficits after approximately 8–10 days of LC activation. In addition, LC activation significantly restored the loss in body weight induced by EAE in the chronic phase ($p < 0.05$, EAE-rM3D_{peak} vs EAE; Fig. 5E).

When the effect of LC activation on spontaneous locomotor activity was explored, there was a significant improvement at 25 dpi ($p < 0.05$), although the AUC score was similar between EAE and EAE-rM3D_{peak} mice (Fig. 5F). Furthermore, no significant differences were found in anxiety-like behavior in the EAE-rM3D_{peak} animals, measured as the time spent in the central area of the open field (Fig. 5G). In terms of the activity/attention score

(See figure on next page.)

Fig. 3 Chronic LC activation from the onset of motor symptoms affects the cortical EAE-associated glial response. Representative images showing astrocyte activation in the **A** PL/IL and **C** M2/M1 cortices, and **B**, **D** the quantification of GFAP immunoreactivity (IR) in arbitrary units (AU). **E–J** Microglial activation reflected by Iba1 immunofluorescence (green) in the **E** PL, **F** IL, **H** M2 and **I** M1 cortices, and **G**, **J** the relative area of these brain regions stained for Iba1. The data represent the mean + SEM and each point corresponds to an individual mouse ($n = 4–5$ per group). [#] $p < 0.01$, ^{###} $p < 0.001$ EAE versus naïve (Additional file 1: Table S4). Scale bars: **A**, **C**, 200 μm ; **E**, **F**, **H**, **I**, 100 μm

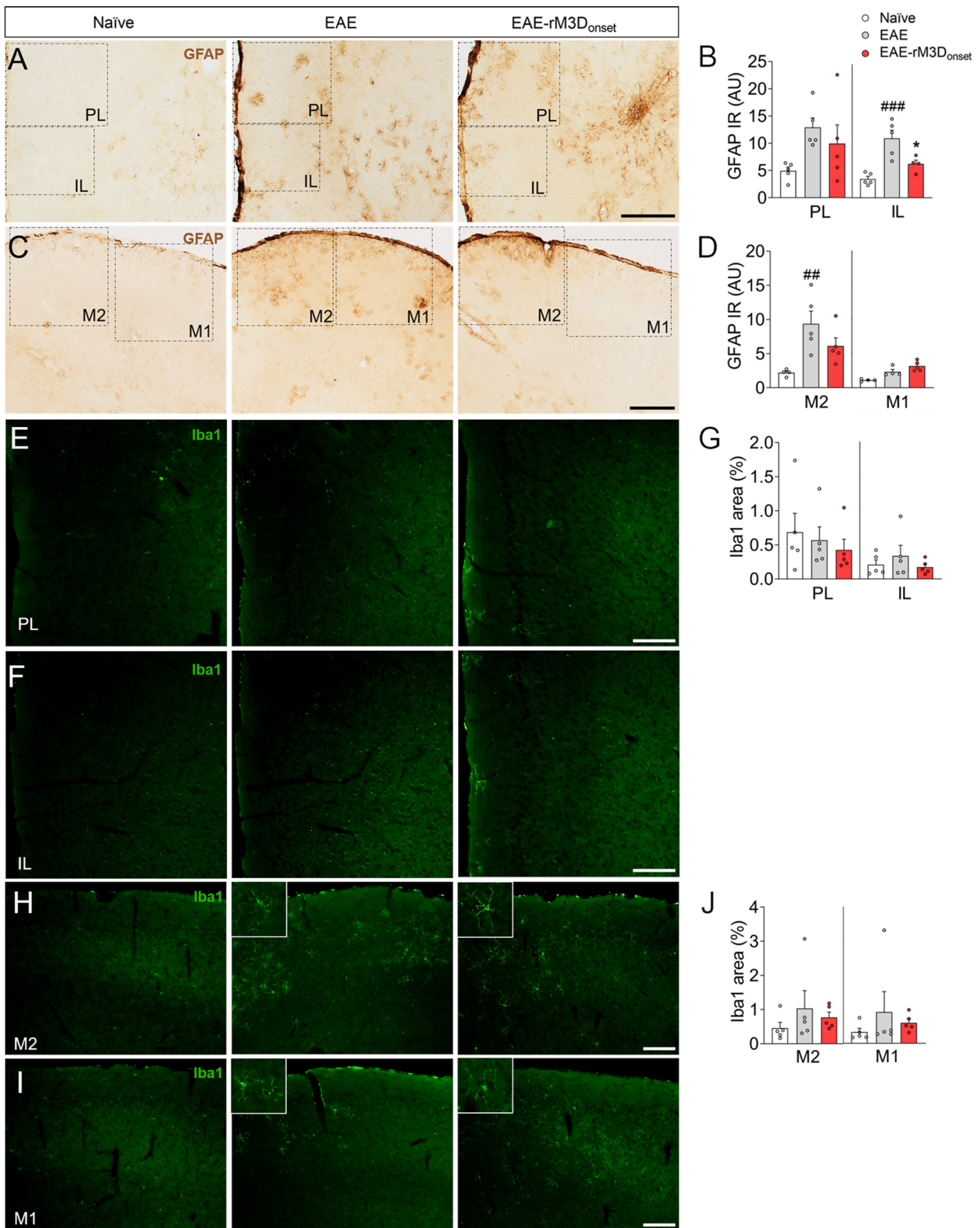


Fig. 3 (See legend on previous page.)

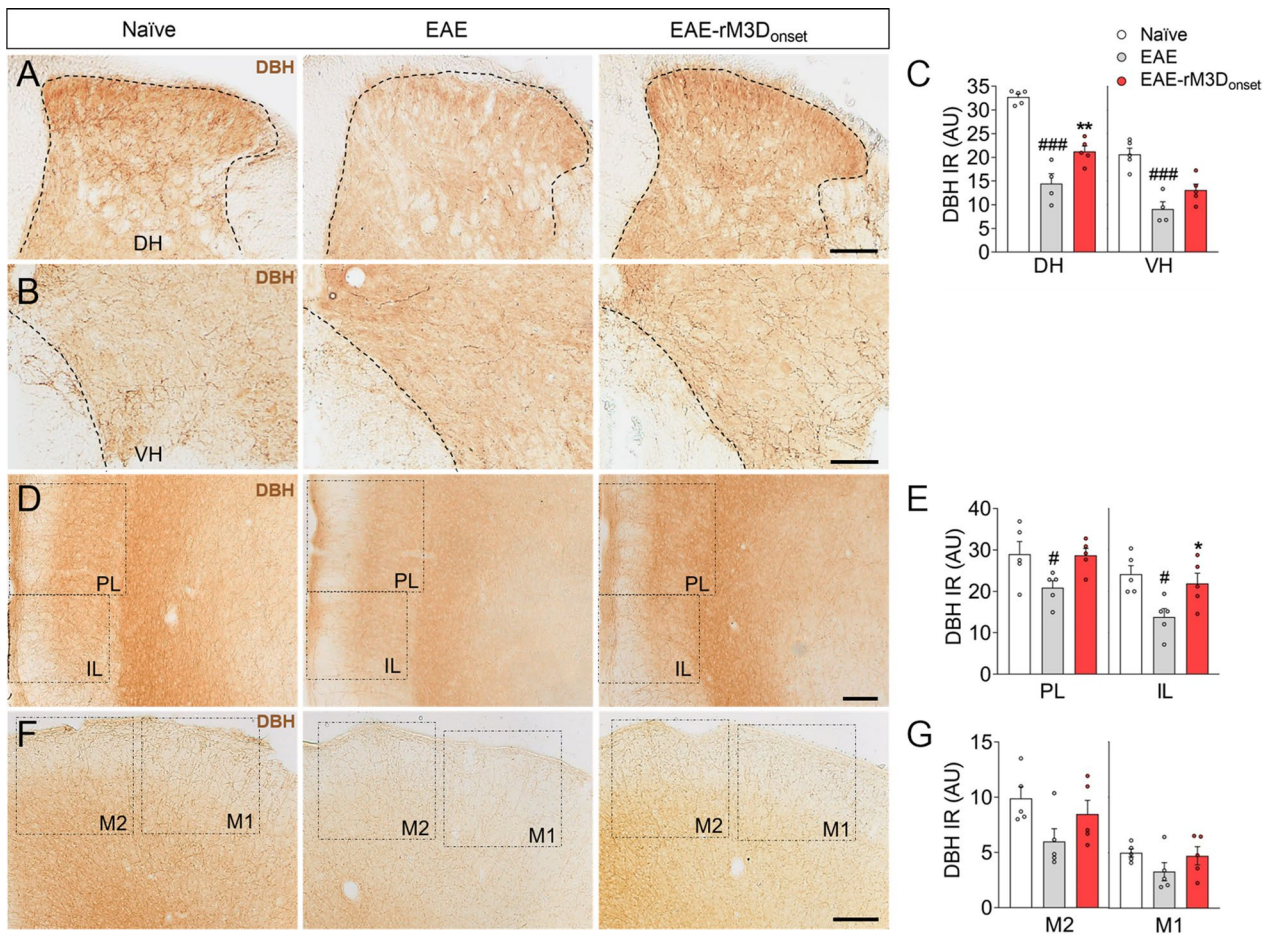


Fig. 4 The effect of early chronic chemogenetic LC activation on noradrenergic projections. Representative images showing DBH-positive fibers in the **A** dorsal and **B** ventral horns (DH, VH) of the lumbar spinal cord, **D** PL/IL and **F** M2/M1 cortices, and **C**, **E**, **G** the quantification of DBH immunoreactivity (IR) in arbitrary units (AU). The data represent the mean + SEM and each point corresponds to an individual mouse ($n=4-5$ per group). # $p < 0.05$, ### $p < 0.001$ EAE versus naïve; * $p < 0.05$, ** $p < 0.01$, EAE-rM3D_{onset} versus EAE (Additional file 1: Table S5). Scale bars: **A**, **B**, **D**, **F**, 100 μm

(Fig. 5H–J), EAE-rM3D_{peak} animals recover the activity/attention score in the chronic phase because they spent less time in this sedentary posture (25 dpi: score: $p < 0.05$; min 4–5, $p < 0.01$; Fig. 5J).

The effects of rM3D(Gs)-DREADD_{peak}-mediated LC activation in the spinal cord

Despite the fact that CNO administration commenced when demyelination was quite advanced (Fig. 6A, B),

(See figure on next page.)

Fig. 5 Chronic LC activation from the peak of motor symptoms affects EAE-induced behavioral alterations. **A** Experimental timeline showing the design of the study to assess the effect of chronic LC activation from the peak of motor symptoms in EAE. Representative images showing mCherry (red) expression in DBH (green) in the LC. Scale bars: 100 μm . **B** Clinical score recorded daily through the course of EAE and their area under the curve (AUC) from the peak of motor deficit and CNO administration (shaded area). **C** The severity of EAE is expressed as the maximum clinical score achieved and **D** percentage change relative to the 17 dpi EAE group, for both the peak (17 dpi) and the chronic (25 dpi) phases of EAE. **E** Body weight over the course of EAE expressed as the relative change from baseline (at the beginning of experiments) and at the end of experiments (29 dpi). **F** The representative activity traces (chronic phase) and the spontaneous locomotor activity expressed as the total distance travelled (arbitrary units, AU), and the AUC from the peak of the motor deficit and CNO administration (shaded area). **G** Representative heat maps (chronic phase) and the relative time spent in the central area of the arena before the onset of motor deficit and CNO administration (10 dpi), at the peak (17 dpi) and chronic (25 dpi) phases of EAE. **H–J** Activity/attention score (above) and the time spent in the sedentary posture (below) at **H** the onset, **I** the peak (17 dpi) and **J** in the chronic (25 dpi) phase of EAE. The data represent the mean + SEM and each point corresponds to an individual mouse ($n=6-10$ per group). # $p < 0.05$, ## $p < 0.01$, ### $p < 0.001$ EAE versus naïve; * $p < 0.05$, ** $p < 0.01$ EAE-rM3D_{onset} versus EAE; &&& $p < 0.001$ EAE-rM3D_{onset} 25 dpi versus 17 dpi (Additional file 1: Table S6). Some elements of this figure were created with [BioRender.com](https://www.biorender.com)

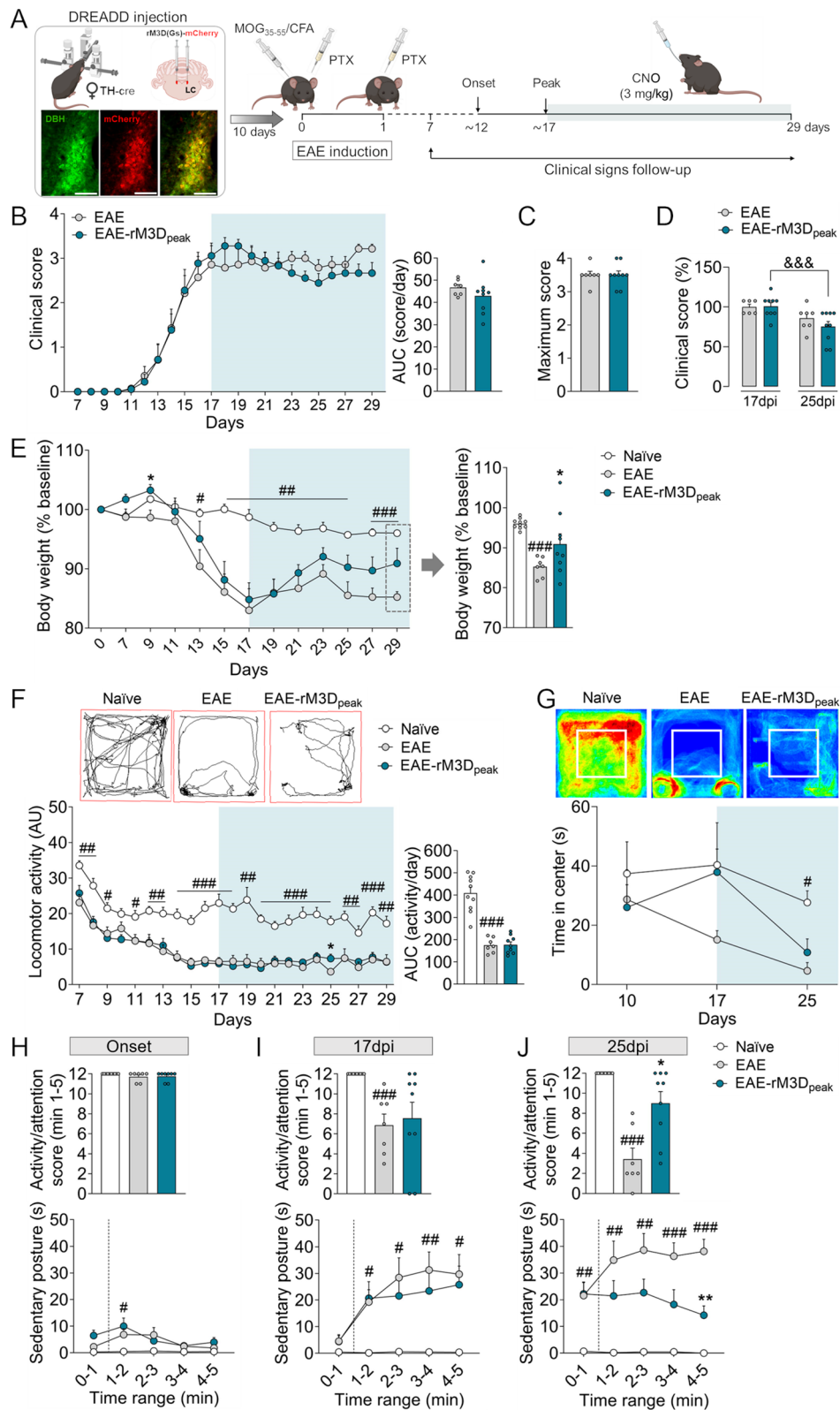


Fig. 5 (See legend on previous page.)

there was a smaller demyelinated area in the ventral white matter of the lumbar spinal cord in EAE-rM3D_{peak} mice than in the EAE animals ($p < 0.01$; Fig. 6B). Furthermore, there was less penetration of perivascular infiltrates along the parenchyma in the thoracic spinal cord of EAE-rM3D_{peak} mice than in EAE animals ($p < 0.05$; Fig. 6C, D). Nevertheless, there were no differences in the number of perivascular cuffs (Fig. 6E, F) or in the number of preclinical perivascular cuffs (Fig. 6G) between EAE-rM3D_{peak} and EAE animals.

As in EAE-rM3D_{onset} mice, GFAP immunoreactivity was weaker in the DH and VH of the lumbar spinal cord in EAE-rM3D_{peak} mice relative to the EAE animals (DH: $p < 0.05$; VH: $p < 0.05$; Fig. 6H–J). Similarly, the relative area occupied by Iba1 in the ventral white matter of the lumbar spinal cord was smaller in EAE-rM3D_{peak} than in the EAE animals ($p < 0.05$; Fig. 6K, L). Finally, there was residual iNOS expression in both EAE and EAE-rM3D_{peak} mice, yet this did not co-localize with Iba1 (Additional file 1: Fig. S3D–F). Furthermore, there were no differences in Arg1 and Iba1 co-localization in EAE-rM3D_{peak} and EAE mice (Fig. 6M–P).

The effects of rM3D(Gs)-DREADD_{peak}-mediated LC activation in the cerebral cortex

We did not observe any significant differences in GFAP expression in the PFC between EAE-rM3D_{peak} and EAE mice (Fig. 7A, B), or in the motor cortex (Fig. 7C, D).

The effect of rM3D(Gs)-DREADD_{peak}-mediated LC activation on noradrenergic projections

Stronger DBH expression was evident in the DH of the spinal cord in EAE-rM3D_{peak} mice relative to the EAE animals ($p < 0.01$; Fig. 7E–G), and in the IL ($p < 0.05$; Fig. 7H, I). However, no significant differences were evident in the M2/M1 cortex of EAE mice relative to the naïve or EAE-rM3D_{peak} animals (Fig. 7J, K). Moreover, a correlation analysis between DBH and GFAP immunoreactivity showed a significant negative correlation in the DH ($p < 0.05$) and VH of the spinal cord ($p < 0.01$; Additional file 1: Fig. S5G–L).

Discussion

The EAE model recapitulates some key aspects of MS and in agreement with previous findings, it provokes time dependent motor weakness and paralysis, as well as other non-motor symptoms. In the CNS, demyelination, inflammation and glial activation in the spinal cord and to a lesser extent in the PFC and motor cortices, was evident in the chronic phase of EAE [37, 38], in conjunction with reduced DBH expression in these areas. Furthermore, enhanced GFAP expression was found in the LC of EAE animals, although the number of TH expressing cells does not change. As previous data demonstrated anti-inflammatory and neuroprotective effects of noradrenaline [15], the enhanced CNS noradrenergic tone after activation of the LC was explored. When chemogenetic LC activation was induced at the onset of motor symptoms, the animal's symptoms improved greatly, such as their anxiety and activity/attention score, as well as their motor deficits. This was accompanied by a clear reversion of demyelination and glial activation in the spinal cord, along with a dampening of the inflammatory parameters, and of DBH expression in the spinal cord and PFC. A second chemogenetic approach involved LC activation when the animals were experiencing more severe paralysis, which demonstrated benefits to animal well-being and a modest alleviation of motor symptoms, as well as an improvement in demyelination and glial activation in the spinal cord, along with an increase in DBH expression in the spinal cord and PFC.

When the possible alterations to the LC induced by EAE were assessed, there was a clear increase in the area of GFAP expression in the LC of EAE animals, which could be related to the role of astrocytes in the neural plasticity that may be induced in the LC projecting areas. However, the number of TH expressing cells remained unaltered at this chronic phase of EAE, consistent with previous findings pointing to an absence of neuronal loss in the LC [9]. When the effect of chemogenetic LC activation was explored from the onset of motor symptoms (~12 dpi), the severity of motor dysfunction induced by EAE was alleviated, as witnessed through the clinical

(See figure on next page.)

Fig. 6 Chronic LC activation from the peak of the EAE motor symptoms affects the spinal cord. **A** Representative images showing the demyelination in the lumbar spinal cord (cyan, MBP) and **B** its quantification expressed as the percentage of area free of MBP in the ventral white matter. **C–G** Perivascular infiltration in the thoracic spinal cord analyzed from **C, E** hematoxylin and eosin staining images and reflected as the **D** infiltration score, **F** perivascular cuffs and **G** preclinical cuffs. **H–J** Representative images showing astrocyte activation in the **H** dorsal and **I** ventral horns (DH, VH) of the lumbar spinal cord, and a graph of the **J** GFAP immunoreactivity (IR) in arbitrary units (AU). **K** Representative immunofluorescence images showing Iba1 (green) expression in the lumbar spinal cord and **L** its quantification, expressed as the relative area of the ventral white matter expressing Iba1. **M–O** Representative immunofluorescence images of Arg1 (red) and Iba1 (green) and corresponding magnifications in the lumbar spinal cord and **P** their quantification, expressed as the percentage of area of the ventral white matter in which Arg1 and Iba1 co-localize relative to the total area occupied by Iba1. The data represent the mean ± SEM and each point corresponds to an individual mouse for **P** that represents a section ($n = 4–5$ per group except for **P**, 15 sections/animal ($n = 3–4$)). $^{##}p < 0.01$; $^{###}p < 0.001$ EAE versus naïve; $^{*}p < 0.05$, $^{**}p < 0.01$ EAE-rM3D_{peak} versus EAE (Additional file 1: Table S7). Scale bars: **A, K, 200** μm; **C, E, H, I, 100** μm; **M, N, O, 50** μm. 250 μm insets in **C**

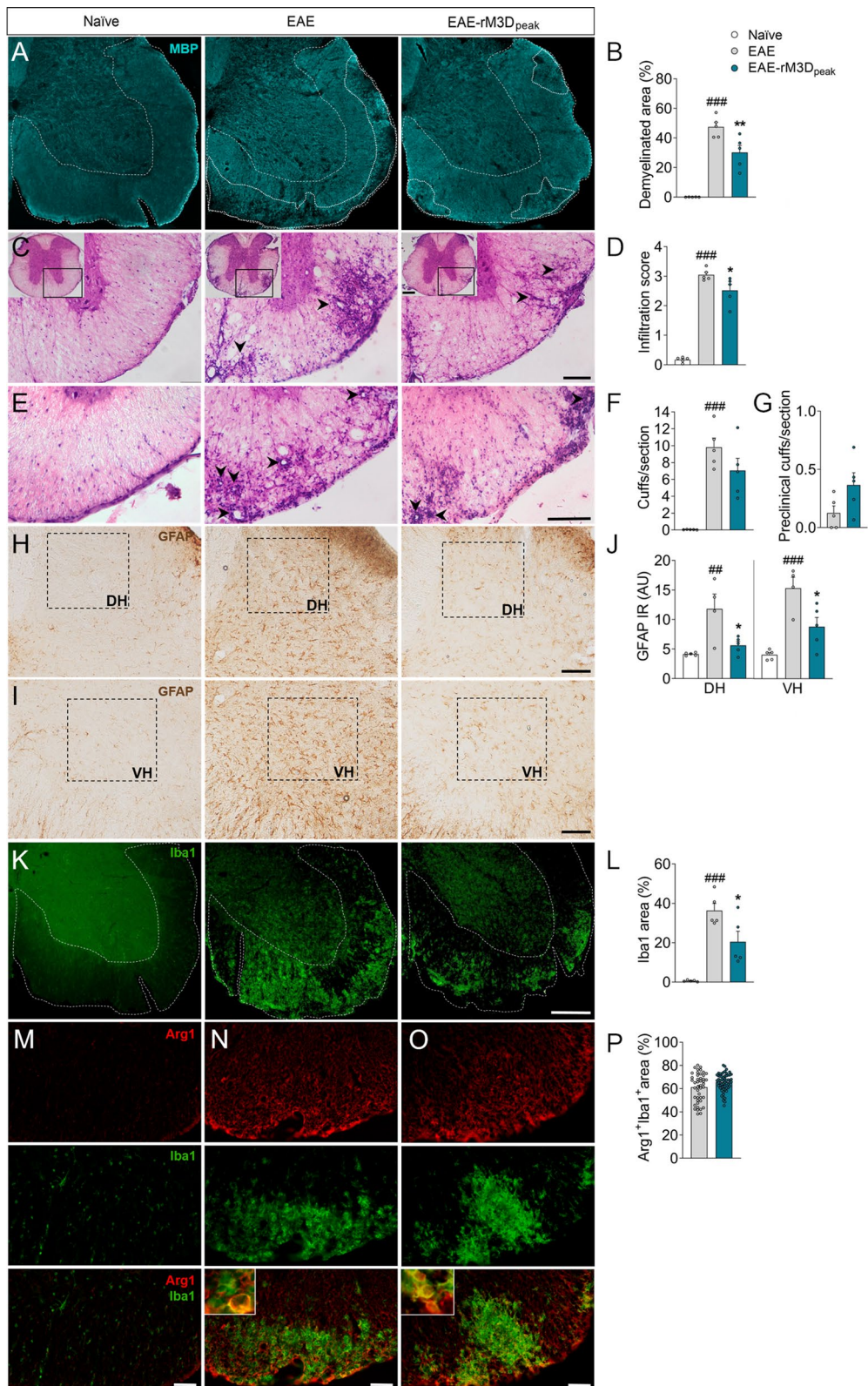


Fig. 6 (See legend on previous page.)

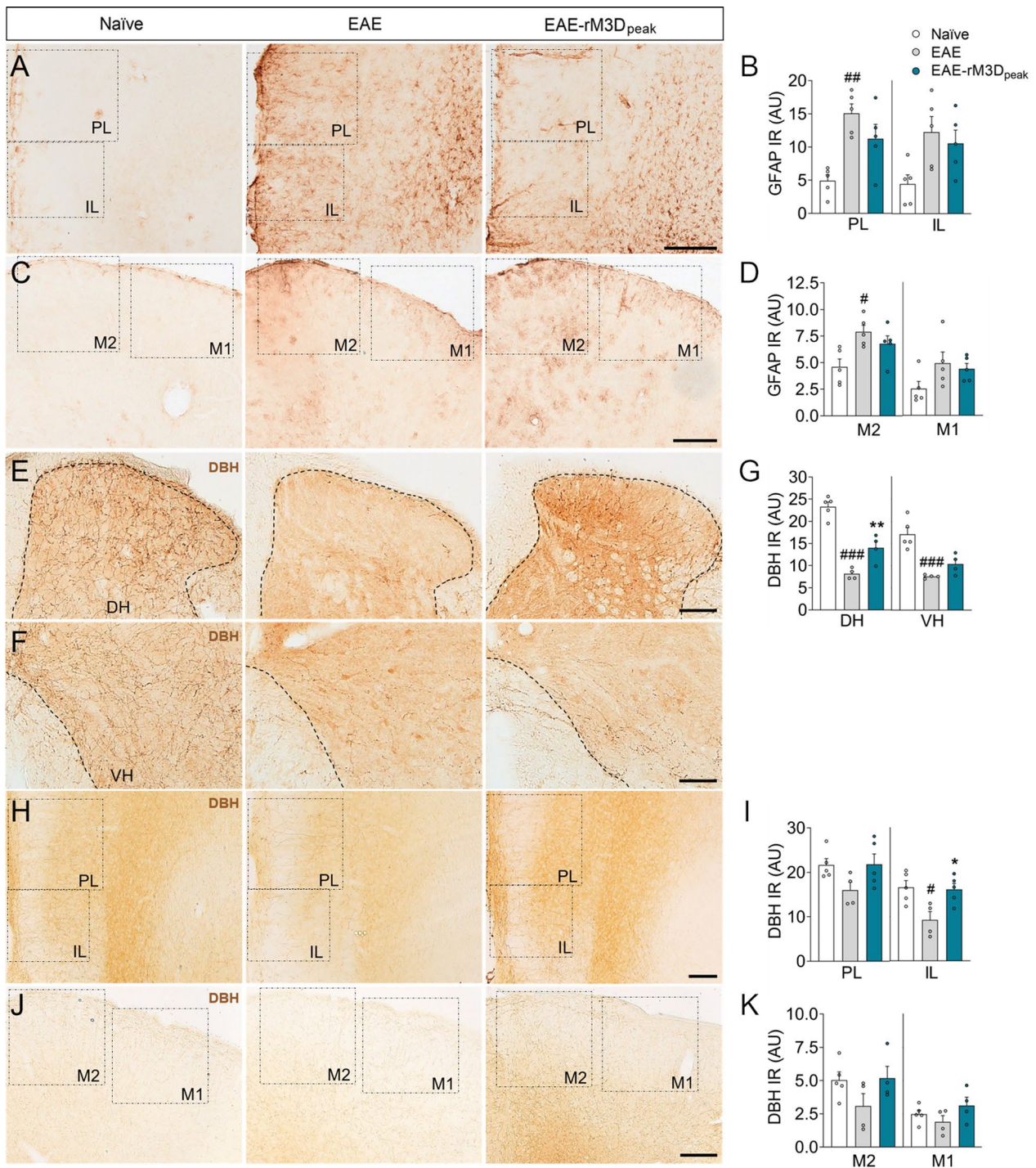


Fig. 7 The effect of late chronic LC activation on cortical astrocyte activation and noradrenergic projections. Representative images showing astrocyte activation in the **A** PL/IL and **C** M2/M1 cortices, and **B**, **D** the quantification of GFAP immunoreactivity (IR) in arbitrary units (AU). Representative images showing DBH positive fibers in **E** the dorsal and **F** ventral horns (DH, VH) of the lumbar spinal cord, **H** PL/IL and **J** M2/M1 cortices, and **G**, **I**, **K** the quantification of DBH IR in AU. The data represent the mean + SEM and each point corresponds to an individual mouse ($n=4-5$ per group). # $p < 0.05$; ## $p < 0.001$ EAE versus naïve; * $p < 0.05$, ** $p < 0.01$ EAE-rM3D_{peak} versus EAE (Additional file 1: Table S8). Scale bars: **A**, **C**, 200 μm ; **E**, **F**, **H**, **J**, 100 μm

score. Spontaneous locomotion was also evaluated in the open field test in which animals can move freely in an arena for 5 min. As expected, the locomotor activity of EAE animals was worse than that of naïve animals as EAE progressed, although it increased significantly in EAE-rM3D_{onset} mice. Interestingly, EAE animals prefer to move to the periphery, avoiding the central anxiogenic area, whereas the EAE-rM3D_{onset} mice better explored the central area, especially after long-term CNO treatment. This is consistent with previous data showing that non-motor symptoms of MS arise, like anxiety [39, 40], and now we show that activation of the LC can help to relieve these alterations. Indeed, this improvement is in agreement with the anxiolytic effect of chronic treatment with noradrenaline enhancing drugs [41, 42]. The activity/attention score was considered a parameter of sickness in rodents and it is significantly reduced in EAE mice [34]. This score is related to the time spent in a specific sedentary posture, reflecting a loss of interest for the environment. This parameter improved considerably in EAE-rM3D_{onset} mice, which spent less time in this sedentary posture both in the peak and chronic phases of EAE. These data indicate that chronic LC activation has a clear beneficial effect on the non-motor symptoms induced by EAE. In addition, LC activation reduced the weight loss induced by EAE, another sign of animal welfare.

One of the most important characteristic of the EAE model is the acute demyelination that contributes to the motor impairment suffered by these mice, which was clearly dampened by rM3D(Gs)-DREADD_{onset}-mediated LC activation. Demyelination is related to the permeabilization of the blood–brain barrier which allows cells from the peripheral immune system to access to the CNS parenchyma [43] as witnessed by the peripheral infiltrates in the spinal cord parenchyma next to venules in EAE animals. However, we found that chronic LC noradrenergic neurons activation reduced the clusters of infiltrates along the parenchyma in the EAE-rM3D_{onset} spinal cord relative to that in EAE mice. The penetration of these infiltrates through the endothelium into the parenchyma is thought to occur in two phases. First, infiltrates pass through the laminin-containing endothelial basement membrane, the membrane proximal to the endothelium. Some days later they penetrate the parenchymal basement membrane, abutting the CNS parenchyma [44, 45] but while the infiltrates gather in the space between these two basement membranes, known as the perivascular space, they form cuffs. These perivascular cuffs can be considered to be clinical if the infiltrates have penetrated the parenchyma or preclinical if they have not yet penetrated the parenchyma. LC activation reduced perivascular infiltration in the spinal cord parenchyma with a predominance in the presence of

preclinical cuffs compared to EAE. Hence, activation of the noradrenergic LC when motor symptoms commence leads to a clear reduction in EAE behavioral symptomatology, while also dampening its pathophysiological progression in terms of spinal cord demyelination and perivascular infiltration.

While glial and immune cells take part in the neuroinflammatory events associated with EAE, either exacerbating or driving their resolution, LC activation dampened the increase in GFAP immunoreactivity in the EAE animal's spinal cord. The area occupied by Iba1 reflects the activated microglia and infiltrated macrophages that tend to migrate to damage zones to remove cellular debris, such as that produced by demyelination [46]. The increase in the relative area occupied by Iba1 in the ventral white matter of the spinal cord in EAE animals was dampened by the LC activation in EAE-rM3D_{onset} animals. This microglial activation was assessed in the relation to the pro-inflammatory marker iNOS or the predominantly anti-inflammatory marker Arg1. Residual iNOS expression was evident in both EAE and EAE-rM3D_{onset} animals but it did not co-localize with Iba1 which suggests that this inflammatory mechanism is not present at this temporal point. Nevertheless, inflammation is thought to fulfill a critical regulatory role in the early stages of EAE, both during the antigen-priming phase and in the subsequent effector phase of the immune response in which the spinal cord is mainly involved [47]. Alternatively, we found enhanced Arg1 expression in spinal cord white matter and stronger colocalization between Arg1 and Iba1 in the EAE-rM3D_{onset} animals than in EAE mice. Thus, LC activation from the onset of motor symptoms may promote the expression of anti-inflammatory markers that contribute to neuroprotection and/or to the resolution of inflammatory events like reactive gliosis. To correlate these behavioral and pathogenic observations with the LC-noradrenergic system, DBH expression was examined in the spinal cord. EAE animals have weaker DBH expression in this tissue and this was echoed by a diminished density of DBH immunoreactive fibers. However, the activation of LC noradrenergic neurons reversed the DBH deficit in the spinal cord (mainly in the DH). Interestingly, a significant negative correlation was found between DBH and GFAP expression in the spinal cord and IL. Hence, the astroglial reaction induced by EAE may be associated with a reduction in DBH expression, such that LC activation was able to counteract this imbalance, suggesting an inverse relationship between glial activation and the lower density of DBH immunoreactive fibers in these areas. This might explain why some therapeutic approaches using noradrenergic precursors are not always effective, such as the use of L-phenylalanine that participates in the DBH

pathway [27, 28], while others do produce positive effects in EAE mice, for example the administration of L-DOPS that is decarboxylated to noradrenaline by endogenous L-aromatic-amino-acid decarboxylase [10]. Therefore, noradrenergic strategies that use alternative DBH routes or that promote DBH activity (such as LC chemogenetics) may be more efficient therapeutic approaches.

In addition to the spinal cord, the PFC (PL and IL) and motor cortices of EAE animals were explored since there is evidence of noradrenaline deficits at cortical levels [9]. Changes in neurodegeneration and glial markers were substantially less severe than in the spinal cord suggesting that these brain areas are better preserved. However, there was a clear reduction in DBH expression in the PL and IL of EAE animals in the chronic phase that seems to be prevented by LC activation in the IL, and more modestly (but not significantly) in the PL. These data are relevant as deficient noradrenergic innervation has been related to anxiodepressive disorders [48], and this may therefore be related to the improvements in sickness behavior and anxiety.

The data obtained agree overall with the previous observations regarding the anti-inflammatory and neuroprotective actions of noradrenaline. Noradrenaline exerts an anti-inflammatory effect through glial cells by attenuating the expression of pro-inflammatory mediators in response to inflammatory events (e.g., TNF- α , IL-1 β , NO, iNOS or NF κ B) [17, 49–53]. Noradrenaline enhancement also promotes neurotrophic support and myelin production through the activation of β 1/2- and α 1-adrenoceptors in astrocytes and oligodendrocytes, respectively [54–56] and it reduces CNS chemokines and cell adhesion molecules expression, molecules that facilitate leucocyte influx into the CNS [57]. These mechanisms triggered by noradrenaline would explain the dampened neuroinflammation and perivascular infiltration observed here after LC noradrenergic activation, as well as the alleviation or prevention of the EAE associated demyelination. Furthermore, modulation of the immune system might be underlying the beneficial effects of noradrenergic tone augmentation. Hence, adrenergic signaling usually acts as a potent suppressive pathway on innate immune cells such as macrophages and dendritic cells [58, 59], mainly through β 2-adrenoceptors, suppressing pro-inflammatory cytokines secretion. Moreover, noradrenaline suppresses toll-like receptor pathways blocking NF κ B activation and increases IL-10 expression that carries out autocrine signaling to block TNF- α and other pro-inflammatory cytokines expression [58–62]. Thus, IL-10 may play a key role in the anti-inflammatory properties of noradrenaline suppressing local and systemic inflammatory processes [62]. On the other hand, noradrenaline and β -agonists are able to regulate T cell

effector functions, for example, suppressing CD8⁺ subsets expression of IFN- γ and TNF- α [63]. Therefore, noradrenaline seems to exert anti-inflammatory effect on immune cells predominantly by its interaction with β -adrenergic receptors.

Once the beneficial effect of chronic LC activation from the onset of motor symptoms was demonstrated in EAE animals, a more challenging approach was adopted to test LC activation from the peak of motor symptoms (~17 dpi), when animals exhibited a robust hind limb paralysis. LC activation for 12–15 days from the peak of motor symptoms only led to a slight alleviation of the motor symptomatology induced by EAE, and although no effect was seen on anxiety, a clear improvement in sickness behavior was evident, as well as an alleviation of body weight loss in the chronic phase of EAE. When exploring demyelination, LC activation significantly reduced the relative size of the demyelinated area in the ventral white matter of the spinal cord, in conjunction with less penetration of perivascular infiltrates along the parenchyma. Nevertheless, no differences in the number of perivascular cuffs or in the number of preclinical perivascular cuffs were found in EAE-rM3D_{peak} mice relative to the EAE animals. As the treatment started at the peak of motor symptoms, infiltration was very advanced and the CNS parenchyma was probably already abutted. However, the treatment seemed to prevent further dissemination of these infiltrates along the CNS parenchyma. Likewise, there was weaker GFAP immunoreactivity in the spinal cord of EAE-rM3D_{peak} animals, which correlates with an increase in DBH_{peak} expression, indicating that beneficial effects induced by LC chemogenetic activation is possible even at advanced stages of EAE progression. Iba1 immunoreactivity in the spinal cord was also weaker in the EAE-rM3D_{peak} mice but it did not co-localize with iNOS. Moreover, the co-expression of Iba1 with Arg1 was similar to that in EAE animals, probably due to LC activation beginning at a later stage of EAE, when inflammation is already advanced. In addition, this chemogenetic LC activation failed to impede cortical EAE-induced GFAP expression even though stronger DBH expression was found in the IL cortex.

Conclusions

These two chemogenetic approaches demonstrated that the noradrenergic LC may be selectively activated even at advanced stages in the evolution of the disease, which suggests that the LC cellular machinery is not so severely affected as in other neurodegenerative pathologies [25]. Although beneficial effects have been achieved through experimental approaches to enhance noradrenaline availability in both preclinical and clinical studies [10, 27, 28, 30, 34, 64–68], we demonstrate here that the selective

activation of LC noradrenergic neurons can alleviate EAE symptomatology. When chemogenetic LC activation starts early, there is a clear neuroprotective and anti-inflammatory effect in the spinal cord, one of the critical areas for the MS, as well as in the IL, which correlates with the benefits to the motor and non-motor symptoms of the disease. The second and more challenging approach arises when the chemogenetic LC activation commences once hind limb paralysis is evident, again producing benefits at the motor and non-motor level that are specifically associated with weaker pathological changes at the spinal cord and IL. It is relevant to note that this treatment is shorter, such that delayed beneficial effects might become evident at later time points. Overall the data suggest that the beneficial effects of the chemogenetic activation of the LC in the context of EAE reflect a potent anti-inflammatory and neuroprotective response. The decrease in reactive gliosis, as well as infiltrated cells and potentiation of the anti-inflammatory response in Iba1⁺ cells, leads to the interpretation of a synergistic signal between the different cell types that converge in a reduction of the pro-inflammatory response and potentiation of the anti-inflammatory one, which facilitates the resolution of the inflammation [15, 69]. Therefore, further studies are necessary to discern how chronic LC activation modulates the pro- or anti-inflammatory profile in EAE along to the identification of the immune populations participating in the therapeutic effect (Th1, Th2, Th17, CD11b, CD45, CD68, CD80, CD163, CD206, MCP1 lymphocytes) that might become key pieces of MS and its clinical management. Finally, this study shows that there is a substantial window of opportunity for LC/noradrenaline-based therapies, even at advance phases of the disease.

Abbreviations

ANOVA	Analysis of variance
AP	Anteroposterior
AU	Arbitrary units
AUC	Area under the curve
Arg1	Arginase-1
CFA	Complete Freund's adjuvant
CNO	Clozapine-N-oxide
CNS	Central nervous system
DBH	Dopamine beta-hydroxylase
DH	Dorsal horn
dpi	Days post EAE induction
DREADD	Designer receptors exclusively activated by designer drugs
EAE	Experimental autoimmune encephalomyelitis
GFAP	Glial fibrillary acidic protein
Iba1	Ionized calcium-binding adapter molecule 1
iNOS	Inducible nitric oxide synthase
IL	Infralimbic cortex
LC	Locus coeruleus
L-DOPS	L-threo-3,4-Dihydroxyphenylserine
M1	Primary motor cortex
M2	Secondary motor cortex
MBP	Myelin basic protein
ML	Midline

MOG _{35–55}	Myelin oligodendrocyte glycoprotein peptide 35–55
MS	Multiple sclerosis
PFC	Prefrontal cortex
PL	Prelimbic cortex
PTX	Pertussis toxin
SEM	Standard error of the mean
TH	Tyrosine hydroxylase
VH	Ventral horn

Supplementary Information

The online version contains supplementary material available at <https://doi.org/10.1186/s12974-023-02865-z>.

Additional file 1. This file includes a detailed description of materials and methods, supplementary figures (Figs. S1–S5) and supplementary tables for antibodies used in this study (Table S1) and summarizing the statistical analysis (Tables S2–S11).

Acknowledgements

We are very grateful to Ms Elena Marín Álvarez for her excellent technical assistance. The Central Services of Scientific and Technological Research, Health Sciences and Animal Research from the University of Cádiz. We also thank Ted Ebendal for providing the mutant mouse B6.129X1-Th^{tm1(cre)}/Kieg, INFRAFRONTIER/EMMA (www.infracorner.eu, PMID: 25414328), and Karolinska Institutet, Stockholm, Sweden, from which the mouse line was distributed (EM:00254).

Author contributions

EB and STS contributed to the study conception and design. EAE induction and behavioral evaluations were performed by STS and JAGP. DREADD technology was performed by MLT. Histological and immunohistochemical assays, the design of protocols for these techniques and image acquisition were conducted by ATC and LB with the contribution of AA. Data collection and analysis were performed by ATC and STS. The manuscript was prepared by EB, STS and ATC with contributions of all other authors. All authors reviewed and approved the manuscript.

Funding

Funding for open access publishing: Universidad de Cádiz/CBUA. This study was supported by the "Fondo Europeo de Desarrollo Regional" (FEDER)-UE "A way to build Europe" from the "Ministerio de Economía y Competitividad" (PID2022-1427850B-I00, PDC2022-133987-I00); from the "Consejería de Transformación Económica, Industria, Conocimiento y Universidad, Junta de Andalucía" (PY20_00958 and CTS-510); from the CEIMAR (CEI-003); from the "Instituto de Investigación e Innovación en Ciencias Biomédicas de Cádiz-INIBICA" (IN-CO9); from the "CIBERSAM": CIBER-Consorcio Centro de Investigación Biomédica en Red (CB07/09/0033), Instituto de Salud Carlos III, Ministerio de Ciencia e Innovación. ATC is a recipient of a FPU fellowship (#FPU20-03072) from "Agencia Estatal de Investigación-Ministerio de Ciencia, Innovación y Universidades".

Availability of data and materials

All datasets used and/or analyzed during the current study are available within the article and its Supplementary Information. Extra information about the data is available on request to the corresponding author.

Declarations

Ethics approval and consent to participate

All animal handling and the procedures were carried out in accordance with the European Commission guidelines (2010/63/EU) and Spanish Law (RD 53/2013) regulating animal research. Moreover, the protocols were approved by the Ethics Committee for Animal Experimentation at the School of Medicine of the University of Cadiz (Spain).

Consent for publication

Not applicable.

Competing interests

The authors declare that they have no competing interests.

Author details

¹Neuropsychopharmacology and Psychobiology Research Group, Department of Neuroscience, University of Cádiz, 11003 Cádiz, Spain. ²Ciber de Salud Mental (CIBERSAM), Instituto de Salud Carlos III, 28029 Madrid, Spain. ³Instituto de Investigación e Innovación Biomédica de Cádiz (INIBICA), Hospital Universitario Puerta del Mar, 11009 Cádiz, Spain. ⁴Neuropsychopharmacology and Psychobiology Research Group, Department of Cell Biology and Histology, University of Cádiz, 11003 Cádiz, Spain. ⁵Department of Biomedicine, Biotechnology and Public Health (Immunology Area), University of Cádiz, 11003 Cádiz, Spain.

Received: 6 June 2023 Accepted: 30 July 2023

Published online: 01 September 2023

References

- Murray TJ. Diagnosis and treatment of multiple sclerosis. *BMJ*. 2006;332(7540):525–7.
- Walton C, King R, Rechtman L, Kaye W, Leray E, Marrie RA, et al. Rising prevalence of multiple sclerosis worldwide: Insights from the Atlas of MS, third edition. *Mult Scler*. 2020;26(14):1816–21.
- The Multiple Sclerosis International Federation. Atlas of MS. 3rd ed. 2020.
- Reich DS, Lucchinetti CF, Calabresi PA. Multiple sclerosis. *N Engl J Med*. 2018;378(2):169–80.
- McGinley MP, Goldschmidt CH, Rae-Grant AD. Diagnosis and treatment of multiple sclerosis: a review. *JAMA*. 2021;325(8):765–79.
- Carandini T, Mancini M, Bogdan I, Rae CL, Barritt AW, Clerico M, et al. In vivo evidence of functional disconnection between brainstem monoaminergic nuclei and brain networks in multiple sclerosis. *Mult Scler Relat Disord*. 2021;56: 103224.
- Carotenuto A, Wilson H, Giordano B, Caminiti SP, Chappell Z, Williams SCR, et al. Impaired connectivity within neuromodulatory networks in multiple sclerosis and clinical implications. *J Neurol*. 2020;267(7):2042–53.
- Gadea M, Martínez-Bisbal MC, Martí-Bonmatí L, Espert R, Casanova B, Coret F, et al. Spectroscopic axonal damage of the right locus coeruleus relates to selective attention impairment in early stage relapsing-remitting multiple sclerosis. *Brain*. 2004;127(Pt 1):89–98.
- Polak PE, Kalinin S, Feinstein DL. Locus coeruleus damage and noradrenaline reductions in multiple sclerosis and experimental autoimmune encephalomyelitis. *Brain*. 2011;134(Pt 3):665–77.
- Simonini MV, Polak PE, Sharp A, McGuire S, Galea E, Feinstein DL. Increasing CNS noradrenaline reduces EAE severity. *J Neuroimmune Pharmacol*. 2010;5(2):252–9.
- Jovanova-Nesić K, Nikolić V, Janković BD. Locus coeruleus and immunity. II. Suppression of experimental allergic encephalomyelitis and hypersensitivity skin reactions in rats with lesioned locus coeruleus. *Int J Neurosci*. 1993;68(3–4):289–94.
- Karpus WJ, Konkol RJ, Killen JA. Central catecholamine neurotoxin administration. 1. Immunological changes associated with the suppression of experimental autoimmune encephalomyelitis. *J Neuroimmunol*. 1988;18(1):61–73.
- Konkol RJ, Wesselmann U, Karpus WJ, Leo GL, Killen JA, Roerig DL. Suppression of clinical weakness in experimental autoimmune encephalomyelitis associated with weight changes, and post-decapitation convulsions after intracisternal-ventricular administration of 6-hydroxydopamine. *J Neuroimmunol*. 1990;26(1):25–34.
- Carnevale D, De Simone R, Minghetti L. Microglia-neuron interaction in inflammatory and degenerative diseases: role of cholinergic and noradrenergic systems. *CNS Neurol Disord Drug Targets*. 2007;6(6):388–97.
- Feinstein DL, Kalinin S, Braun D. Causes, consequences, and cures for neuroinflammation mediated via the locus coeruleus: noradrenergic signaling system. *J Neurochem*. 2016;139(Suppl 2):154–78.
- Galea E, Heneka MT, Dello Russo C, Feinstein DL. Intrinsic regulation of brain inflammatory responses. *Cell Mol Neurobiol*. 2003;23(4–5):625–35.
- Madrigal JL, Feinstein DL, Dello Russo C. Norepinephrine protects cortical neurons against microglial-induced cell death. *J Neurosci Res*. 2005;81(3):390–6.
- Berridge CW. Noradrenergic modulation of arousal. *Brain Res Rev*. 2008;58(1):1–17.
- Del Campo N, Chamberlain SR, Sahakian BJ, Robbins TW. The roles of dopamine and noradrenaline in the pathophysiology and treatment of attention-deficit/hyperactivity disorder. *Biol Psychiatry*. 2011;69(12):e145–57.
- Montoya A, Bruins R, Katzman MA, Blier P. The noradrenergic paradox: implications in the management of depression and anxiety. *Neuropsychiatr Dis Treat*. 2016;12:541–57.
- Suárez-Pereira I, Llorca-Torralba M, Bravo L, Camarena-Delgado C, Soriano-Mas C, Berrocoso E. The role of the locus coeruleus in pain and associated stress-related disorders. *Biol Psychiatry*. 2022;91(9):786–97.
- Chen Y, Chen T, Hou R. Locus coeruleus in the pathogenesis of Alzheimer's disease: a systematic review. *Alzheimers Dement (N Y)*. 2022;8(1): e12257.
- Kelly SC, He B, Perez SE, Ginsberg SD, Mufson EJ, Counts SE. Locus coeruleus cellular and molecular pathology during the progression of Alzheimer's disease. *Acta Neuropathol Commun*. 2017;5(1):8.
- Madelung CF, Meder D, Fuglsang SA, Marques MM, Boer VO, Madsen KH, et al. Locus coeruleus shows a spatial pattern of structural disintegration in Parkinson's disease. *Mov Disord*. 2022;37(3):479–89.
- Weinschenker D. Long road to ruin: noradrenergic dysfunction in neurodegenerative disease. *Trends Neurosci*. 2018;41(4):211–23.
- Pacheco R, Contreras F, Zouali M. The dopaminergic system in autoimmune diseases. *Front Immunol*. 2014;5:117.
- Loder C, Allawi J, Horrobin DF. Treatment of multiple sclerosis with lofepramine, L-phenylalanine and vitamin B(12): mechanism of action and clinical importance: roles of the locus coeruleus and central noradrenergic systems. *Med Hypotheses*. 2002;59(5):594–602.
- Wade DT, Young CA, Chaudhuri KR, Davidson DL. A randomised placebo controlled exploratory study of vitamin B-12, lofepramine, and L-phenylalanine (the "Cari Loder regime") in the treatment of multiple sclerosis. *J Neurol Neurosurg Psychiatry*. 2002;73(3):246–9.
- Li Q, Yang T, Guo AC, Fan YP. Role of catalpol in ameliorating the pathogenesis of experimental autoimmune encephalomyelitis by increasing the level of noradrenaline in the locus coeruleus. *Mol Med Rep*. 2018;17(3):4163–72.
- Polak PE, Kalinin S, Braun D, Sharp A, Lin SX, Feinstein DL. The vincamine derivative vindeburnol provides benefit in a mouse model of multiple sclerosis: effects on the locus coeruleus. *J Neurochem*. 2012;121(2):206–16.
- Sciolino NR, Plummer NW, Chen YW, Alexander GM, Robertson SD, Dudek SM, et al. Recombinase-dependent mouse lines for chemogenetic activation of genetically defined cell types. *Cell Rep*. 2016;15(11):2563–73.
- INFRAFRONTIER Consortium. INFRAFRONTIER—providing mutant mouse resources as research tools for the international scientific community. *Nucleic Acids Res*. 2015;43(Database issue):D1171–5.
- Paxinos G, Franklin KBJ. *The Mouse Brain in Stereotaxic Coordinates*, 5th edn, Paxinos G, ed. Amsterdam: Elsevier; 2019.
- Musgrave T, Benson C, Wong G, Browne I, Tenorio G, Rauw G, et al. The MAO inhibitor phenelzine improves functional outcomes in mice with experimental autoimmune encephalomyelitis (EAE). *Brain Behav Immun*. 2011;25(8):1677–88.
- An K, Xue MJ, Zhong JY, Yu SN, Lan TS, Qi ZQ, et al. Arsenic trioxide ameliorates experimental autoimmune encephalomyelitis in C57BL/6 mice by inducing CD4. *J Neuroinflammation*. 2020;17(1):147.
- Yakimov V, Schweiger F, Zhan J, Behrangi N, Horn A, Schmitz C, et al. Continuous cuprizone intoxication allows active experimental autoimmune encephalomyelitis induction in C57BL/6 mice. *Histochem Cell Biol*. 2019;152(2):119–31.
- Brown DA, Sawchenko PE. Time course and distribution of inflammatory and neurodegenerative events suggest structural bases for the pathogenesis of experimental autoimmune encephalomyelitis. *J Comp Neurol*. 2007;502(2):236–60.
- Day MJ. Histopathology of EAE. In: Lavi E, Constantinescu CS, editors. *Experimental models of multiple sclerosis*. Boston: Springer; 2005. p. 25–43.

39. Marrie RA, Horwitz R, Cutter G, Tyry T, Campagnolo D, Vollmer T. The burden of mental comorbidity in multiple sclerosis: frequent, underdiagnosed, and undertreated. *Mult Scler*. 2009;15(3):385–92.
40. Peruga I, Hartwig S, Thöne J, Hovemann B, Gold R, Juckel G, et al. Inflammation modulates anxiety in an animal model of multiple sclerosis. *Behav Brain Res*. 2011;220(1):20–9.
41. Bodnoff SR, Suranyi-Cadotte B, Aitken DH, Quirion R, Meaney MJ. The effects of chronic antidepressant treatment in an animal model of anxiety. *Psychopharmacology*. 1988;95(3):298–302.
42. Troelsen KB, Nielsen E, Mirza NR. Chronic treatment with duloxetine is necessary for an anxiolytic-like response in the mouse zero maze: the role of the serotonin transporter. *Psychopharmacology*. 2005;181(4):741–50.
43. Shechter R, Schwartz M. Harnessing monocyte-derived macrophages to control central nervous system pathologies: no longer “if” but “how.” *J Pathol*. 2013;229(2):332–46.
44. Agrawal SM, Williamson J, Sharma R, Kebir H, Patel K, Prat A, et al. Extracellular matrix metalloproteinase inducer shows active perivascular cuffs in multiple sclerosis. *Brain*. 2013;136(Pt 6):1760–77.
45. Toft-Hansen H, Buist R, Sun XJ, Schellenberg A, Peeling J, Owens T. Metalloproteinases control brain inflammation induced by pertussis toxin in mice overexpressing the chemokine CCL2 in the central nervous system. *J Immunol*. 2006;177(10):7242–9.
46. Sen MK, Mahns DA, Coorsen JR, Shortland PJ. The roles of microglia and astrocytes in phagocytosis and myelination: Insights from the cuprizone model of multiple sclerosis. *Glia*. 2022;70(7):1215–50.
47. Sonar SA, Lal G. The iNOS activity during an immune response controls the CNS pathology in experimental autoimmune encephalomyelitis. *Front Immunol*. 2019;10:710.
48. Gonzalez MM, Aston-Jones G. Light deprivation damages monoamine neurons and produces a depressive behavioral phenotype in rats. *Proc Natl Acad Sci U S A*. 2008;105(12):4898–903.
49. Dello Russo C, Boullenne AI, Gavriluk V, Feinstein DL. Inhibition of microglial inflammatory responses by norepinephrine: effects on nitric oxide and interleukin-1beta production. *J Neuroinflammation*. 2004;1(1):9.
50. Feinstein DL, Galea E, Reis DJ. Norepinephrine suppresses inducible nitric oxide synthase activity in rat astroglial cultures. *J Neurochem*. 1993;60(5):1945–8.
51. Gavriluk V, Horvath P, Weinberg G, Feinstein DL. A 27-bp region of the inducible nitric oxide synthase promoter regulates expression in glial cells. *J Neurochem*. 2001;78(1):129–40.
52. Hinojosa AE, Caso JR, Garcia-Bueno B, Leza JC, Madrigal JL. Dual effects of noradrenaline on astroglial production of chemokines and pro-inflammatory mediators. *J Neuroinflammation*. 2013;10:81.
53. Jiang L, Chen SH, Chu CH, Wang SJ, Oyarzabal E, Wilson B, et al. A novel role of microglial NADPH oxidase in mediating extra-synaptic function of norepinephrine in regulating brain immune homeostasis. *Glia*. 2015;63(6):1057–72.
54. Juric DM, Miklic S, Carman-Krzan M. Monoaminergic neuronal activity up-regulates BDNF synthesis in cultured neonatal rat astrocytes. *Brain Res*. 2006;1108(1):54–62.
55. Juric DM, Loncar D, Carman-Krzan M. Noradrenergic stimulation of BDNF synthesis in astrocytes: mediation via alpha1- and beta1/beta2-adrenergic receptors. *Neurochem Int*. 2008;52(1–2):297–306.
56. Davis H, Guo X, Lambert S, Stancescu M, Hickman JJ. Small molecule induction of human umbilical stem cells into MBP-positive oligodendrocytes in a defined three-dimensional environment. *ACS Chem Neurosci*. 2012;3(1):31–9.
57. O’Sullivan JB, Ryan KM, Harkin A, Connor TJ. Noradrenaline reuptake inhibitors inhibit expression of chemokines IP-10 and RANTES and cell adhesion molecules VCAM-1 and ICAM-1 in the CNS following a systemic inflammatory challenge. *J Neuroimmunol*. 2010;220(1–2):34–42.
58. Grailer JJ, Haggadone MD, Sarma JV, Zetoune FS, Ward PA. Induction of M2 regulatory macrophages through the beta2-adrenergic receptor with protection during endotoxemia and acute lung injury. *J Innate Immun*. 2014;6(5):607–18.
59. Donnelly LE, Tudhope SJ, Fenwick PS, Barnes PJ. Effects of formoterol and salmeterol on cytokine release from monocyte-derived macrophages. *Eur Respir J*. 2010;36(1):178–86.
60. Ağaç D, Estrada LD, Maples R, Hooper LV, Farrar JD. The beta2-adrenergic receptor controls inflammation by driving rapid IL-10 secretion. *Brain Behav Immun*. 2018;74:176–85.
61. Kizaki T, Shirato K, Sakurai T, Ogasawara JE, Oh-ishi S, Matsuoka T, et al. Beta2-adrenergic receptor regulate Toll-like receptor 4-induced late-phase NF-kappaB activation. *Mol Immunol*. 2009;46(6):1195–203.
62. Sharma D, Farrar JD. Adrenergic regulation of immune cell function and inflammation. *Semin Immunopathol*. 2020;42(6):709–17.
63. Estrada LD, Ağaç D, Farrar JD. Sympathetic neural signaling via the beta2-adrenergic receptor suppresses T-cell receptor-mediated human and mouse CD8(+) T-cell effector function. *Eur J Immunol*. 2016;46(8):1948–58.
64. Benson CA, Wong G, Tenorio G, Baker GB, Kerr BJ. The MAO inhibitor phenelzine can improve functional outcomes in mice with established clinical signs in experimental autoimmune encephalomyelitis (EAE). *Behav Brain Res*. 2013;252:302–11.
65. Berne-Fromell K, Fromell H, Lundkvist S, Lundkvist P. Is multiple sclerosis the equivalent of Parkinson’s disease for noradrenaline? *Med Hypotheses*. 1987;23(4):409–15.
66. Puri BK, Bydder GM, Chaudhuri KR, Al Saffar BY, Curati WL, White SJ, et al. MRI changes in multiple sclerosis following treatment with lofepramine and L-phenylalanine. *NeuroReport*. 2001;12(9):1821–4.
67. Solaro C, Bergamaschi R, Rezzani C, Mueller M, Trabucco E, Bargiggia V, et al. Duloxetine is effective in treating depression in multiple sclerosis patients: an open-label multicenter study. *Clin Neuropharmacol*. 2013;36(4):114–6.
68. Vollmar P, Nessler S, Kalluri SR, Hartung HP, Hemmer B. The antidepressant venlafaxine ameliorates murine experimental autoimmune encephalomyelitis by suppression of pro-inflammatory cytokines. *Int J Neuropsychopharmacol*. 2009;12(4):525–36.
69. Braun D, Madrigal JL, Feinstein DL. Noradrenergic regulation of glial activation: molecular mechanisms and therapeutic implications. *Curr Neuropharmacol*. 2014;12(4):342–52.

Publisher’s Note

Springer Nature remains neutral with regard to jurisdictional claims in published maps and institutional affiliations.

Ready to submit your research? Choose BMC and benefit from:

- fast, convenient online submission
- thorough peer review by experienced researchers in your field
- rapid publication on acceptance
- support for research data, including large and complex data types
- gold Open Access which fosters wider collaboration and increased citations
- maximum visibility for your research: over 100M website views per year

At BMC, research is always in progress.

Learn more biomedcentral.com/submissions

